

## Gibbs-ensemble path-integral Monte Carlo simulations of a mixed quantum-classical fluid

F. Schneider,<sup>1</sup> D. Marx,<sup>2,\*</sup> and P. Nielaba<sup>1</sup>

<sup>1</sup>*Institut für Physik, Johannes Gutenberg-Universität, KoMa 331, D-55099 Mainz, Germany*

<sup>2</sup>*IBM Research Division, Zurich Research Laboratory, Säumerstrasse 4, CH-8803 Rüschlikon, Switzerland*

(Received 7 September 1994)

We study a model fluid with classical translational degrees of freedom and internal quantum states in two spatial dimensions. The path-integral Monte Carlo and the Gibbs-ensemble Monte Carlo techniques are combined to investigate the liquid-gas coexistence region in this mixed quantum-classical system. A comparison with the phase diagram obtained in the canonical ensemble is also presented.

PACS number(s): 64.70.Fx, 61.20.Ja, 05.30.-d, 75.10.Jm

Monte Carlo (MC) simulations in the Gibbs ensemble [1,2] have now been successfully used for several years to study first-order phase transitions in fluids; for recent reviews see [3]. For temperatures far below the critical point, satisfactory results for the phase coexistence densities can be obtained. Near the critical point, however, finite size effects become significant, and finite size scaling [4] has proven to be important in the study of off-lattice systems [5]. Recently, phase transitions in two-dimensional systems [6] have received much attention in experimental studies of phase transitions in adsorbed layers [7] as well as in MC studies [8], in particular phase transitions at low temperatures where quantum effects become important. In this regime it is often a satisfactory approximation to treat only a subset of all degrees of freedom on a quantum-mechanical basis. Thus generic Hamiltonians for such problems often contain classical and quantum degrees of freedom.

Until now, simulations in the Gibbs-ensemble have been applied to purely classical systems. In this paper we present a Gibbs-ensemble Monte Carlo (GEMC) study of phase coexistence in a two-dimensional fluid with internal quantum states using path-integral Monte Carlo (PIMC) techniques [9]; for a review of PIMC see [10]. In the present paper we will focus on the liquid-gas envelope, the main domain of applicability of the GEMC technique. In our previous canonical PIMC simulations [11] this coexistence region as well as the solid coexistence density were mapped by exploiting the off-lattice generalization [5] of the block analysis method [4]. The two-dimensional fluid to be defined below serves as a generic model for a certain class of physisorbed molecules. It exhibits astonishingly rich phase behavior including various liquid-gas-solid coexistences, a critical line ending in a tricritical point, as well as two solid phases with two associated triple points. Many *qualitative* features observed in real systems are obtained, although we had not intended to model any specific adsorbate, see [12].

In particular, we study the liquid-gas transition of a model fluid with internal quantum states [11,13,14]. Its mixed quantum-classical Hamiltonian is given by

$$H = \sum_{i=1}^N \frac{\mathbf{p}_i^2}{2M} - \frac{\omega_0}{2} \sum_{i=1}^N \sigma_i^x + \sum_{i<j} U(r_{ij}) - \sum_{i<j} J(r_{ij}) \sigma_i^z \sigma_j^z, \quad (1)$$

where  $M$  is the particle mass,  $\mathbf{p}_i$  is the momentum of particle  $i$ ,  $r_{ij}$  is the distance between particles  $i$  and  $j$ , and  $\sigma^x$  and  $\sigma^z$  are the usual Pauli spin half-matrices. The potential energy consists of a one-particle (two-level) part with tunnel splitting  $\omega_0$  and two pair interaction terms  $U(r)$  and  $J(r)$ . We chose  $U(r)$  to be a hard disk potential for particles with diameter  $d$  and  $J(r)$  to be a square well potential with  $J(r) = J$  for  $d < r < 1.5d$  and zero elsewhere. The total number of particles  $N$  and the total volume  $V$  is fixed; the average dimensionless density is  $\bar{\rho}^* = \rho d^2$ . The particles are constrained to move in two spatial dimensions, which mimics an adsorbate in the strong-adsorption-small-corrugation limit. In the adiabatic approximation we assume a separation of the translational and internal degrees of freedom and treat the translations classically, which is justified for large particle masses  $M$ .

Application of the Trotter formula [10] results in the following expression for the system's partition function  $Z(\beta, N, V)$  in the Gibbs ensemble:

$$\begin{aligned} Z(\beta, N, V) &= \lim_{P \rightarrow \infty} Z_P(\beta, N, V) \\ &= \lim_{P \rightarrow \infty} \sum_{N_1=0}^N \int_0^V dV_1 Z_P(\beta, N_1, V_1) \\ &\quad \times Z_P(\beta, N_2, V_2) \end{aligned} \quad (2)$$

at temperature  $T^* = (\beta J)^{-1}$  with the discretized partition function in the GEMC box  $k$  for fixed Trotter dimension  $P$  being

$$\begin{aligned} Z_P(\beta, N_k, V_k) &= \frac{A_P^{N_k P}}{\lambda^{2N_k} N_k!} \int d\mathbf{r}^{N_k} \exp \left[ -\beta \sum_{i<j} U(r_{ij}) \right] \\ &\quad \times \sum_{\{S\}} \exp \left[ -\beta \left\{ W_{\text{eff}}^{x,k}(\{S\}, \{r\}) \right. \right. \\ &\quad \left. \left. + W_{\text{eff}}^{z,k}(\{S\}, \{r\}) \right\} \right]. \end{aligned} \quad (3)$$

Here  $N_k$  denotes the number of particles in the GEMC box  $k$  with volume  $V_k$ ,  $k \in \{1, 2\}$ , and the  $NVT$ -GEMC constraints [3]  $N_1 + N_2 = N$  and  $V_1 +$

\*Present address: Max-Planck-Institut für Festkörperforschung, Heisenbergstrasse 1, D-70569 Stuttgart, Germany.

$V_2 = V$  have to be satisfied for each configuration.  $W_{\text{eff}}^{x,k}(\{S\}, \{r\}) = -\sum_{i=1}^{N_k} \sum_{p=1}^P K_P S_{i,p} S_{i,p+1}$  denotes the effective *intramolecular* potential and  $W_{\text{eff}}^{z,k}(\{S\}, \{r\}) = -\sum_{i<j}^{N_k} \sum_{p=1}^P \frac{1}{P} J(r_{ij}) S_{i,p} S_{j,p}$  denotes the effective *intermolecular* potential with the pseudospin variables  $S_{i,p} = \pm 1$ . Moreover, in the GEMC simulation all necessary volume and particle decompositions have to be taken into account properly for the full partition function [15]. The temperature-dependent coefficients  $A_P$  and  $K_P$  are given by  $A_P = [\frac{1}{2} \sinh(\beta\omega_0/P)]^{1/2}$  and  $K_P = \frac{1}{2\beta} \ln[\coth(\beta\omega_0/2P)]$  where  $\lambda$  denotes the thermal de Broglie wavelength and the quantum chains have to satisfy periodic boundary conditions with respect to  $P$ .

We study several thermal properties of the model defined in Eq. (1) by averaging observables using the Boltzmann factor resulting from the mapping of the original quantum problem to the corresponding equivalent classical system. In particular we study in both simulation boxes  $k$  the properties of the magnetization  $m_k$  as averages along the quantum chains,  $m_k := \langle \sum_{i=1}^{N_k} \sum_{p=1}^P S_{i,p} / N_k P \rangle_k$ , the (dimensionless) interaction energy  $E_k^z$  per particle,  $E_k^z := \beta \langle W_{\text{eff}}^{z,k}(\{S\}, \{r\}) / N_k \rangle_k$ , the dimensionless internal energy  $E_k^x$  per particle,

$$E_k^x := -(\beta\omega_0/2) \left[ \tanh^{-1}(\beta\omega_0/P) + \{PK_P \sinh(\beta\omega_0/P)\}^{-1} \times \langle W_{\text{eff}}^{x,k}(\{S\}, \{r\}) / N_k \rangle_k \right], \quad (4)$$

and the particle density  $\rho_k^*$ . Here  $\langle \rangle_k$  denotes the standard average in box  $k$  of the Gibbs ensemble [1] for the mixed quantum-classical Hamiltonian. We shall henceforth omit the box index of the thermal averages and refer directly to the boxes.

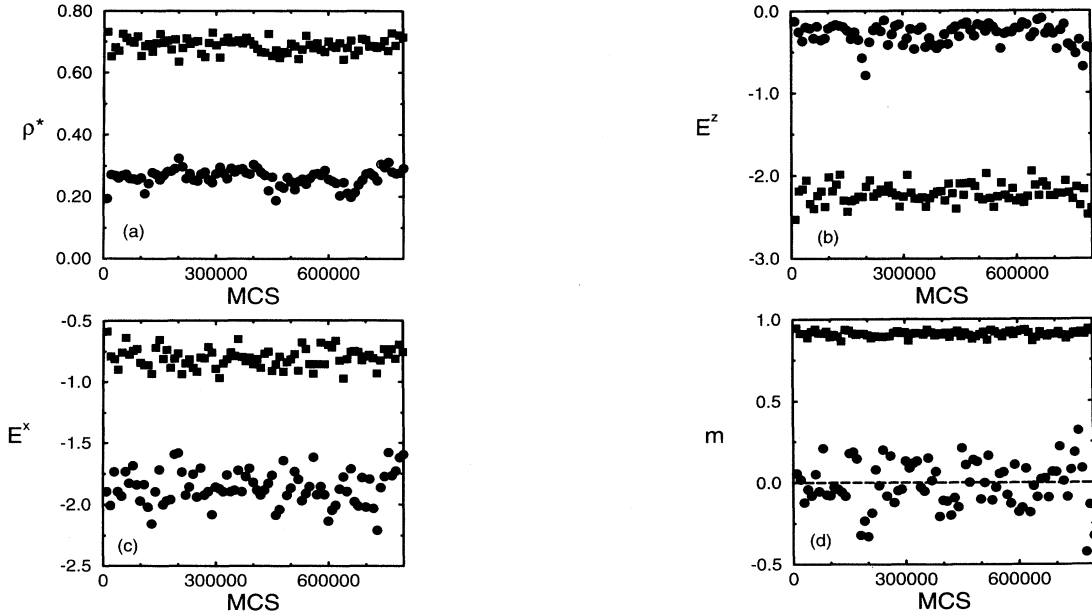


FIG. 2. (a) Time evolution of density, (b) interaction energy  $E^z$ , (c) internal energy  $E^x$ , and (d) magnetization at temperature  $T^* = 0.45$  and density  $\bar{\rho}^* = 0.45$ . Squares indicate the results in box 1, circles in box 2.

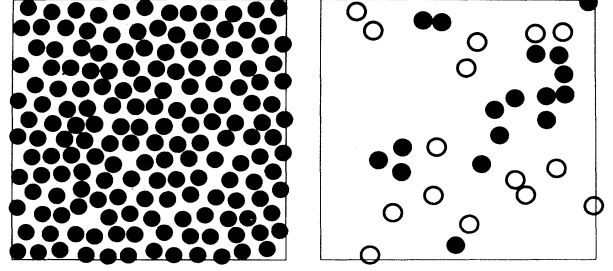


FIG. 1. Snapshot of configurations in the two simulation boxes at  $T^* = 0.35$  and  $\bar{\rho}^* = 0.45$ . The instantaneous magnetic moment of the particles  $\mu_i = \sum_{p=1}^P S_{i,p} / P$  is represented by solid ( $\mu_i > 0$ ) and empty ( $\mu_i < 0$ ) circles.

In order to study the systematic ensemble dependencies of the liquid-gas coexistence densities, which recently received much attention in the context of GEMC simulations [17,18], we chose the same parameters as in [11]. Thus the Gibbs ensemble simulations [15,16] were performed for  $\omega_0/J = 4$  (where  $J = 1$ ) with  $N = 200$  particles and a Trotter dimension chosen to satisfy  $P/\beta J \approx 40$  for each temperature.

In addition to many other phase transitions [11], at low temperatures the system undergoes a first-order transition with coexistence between a paramagnetic gas and a ferromagnetic liquid. This liquid-gas transition is the focus of the present work in the Gibbs ensemble. In Fig. 1 we show a typical snapshot of the configurations in the two boxes at an average density of  $\bar{\rho}^* = 0.45$  and temperature  $T^* = 0.35$ . The system is deep in the two-phase coexistence regime: one box contains a paramagnetic gas and the other contains simultaneously a dense ferromagnetic liquid. In Fig. 2 we present the results for densities, magnetizations, and internal and interaction energies in the two boxes as a function of MC steps at  $T^* = 0.45$  and  $\bar{\rho}^* = 0.45$ . For these parameters we obtain a clear phase

separation into a phase at high density and high magnetization in box 1 and a phase at low density and low magnetization in box 2. In the gas box 2 the particles are mainly in their  $\sigma^x$  ground states, the internal energy  $E^x$  is small, and the magnetic interaction energy  $E^z$  is nearly zero. In box 1, however, the particles are hybridized and occupy to a large extent  $\sigma^z$  eigenstates, resulting in a large value for their individual magnetic moments and thus for the total magnetization  $m$  in that liquid phase. The higher density leads to small interparticle distances and thus to a low interaction energy and an internal energy that is much larger than that in box 2. Note that the Gibbs-ensemble technique [3] gives immediate and simple access to such thermal properties of the coexisting phases (as long as the boxes do not exchange identity, see below), whereas the block analysis technique [5,11,19] is tailored to yield the distribution function of the order parameter, i.e., the density in this case. Histograms for magnetization and density are presented in Figs. 3(a) and 3(b), respectively. At low temperatures the two phases are quite stable in the two boxes, where the average magnetization in box 1 decreases with increasing temperature as well as with the density difference between the two boxes. At temperatures close to  $T^* \approx 0.55$  the system is near its liquid-gas critical point, which is a tricritical point due to the merging of the magnetic critical line into the liquid-gas coexistence curve. In this case the time evolutions of observables are not as stable as in Fig. 2. Owing to the increasing correlation length which exceeds that of the simulation boxes, the identities of the two boxes change often, resulting in overlaps of the density and magnetization histograms. In the case of clearly separated peaks in the density histograms [see Fig. 3(b)], the coexistence densities are easily obtained by computing the first moments of these distributions. In the case of histograms with a double peak structure, the coexistence densities are obtained by fitting “half” Gaussians to

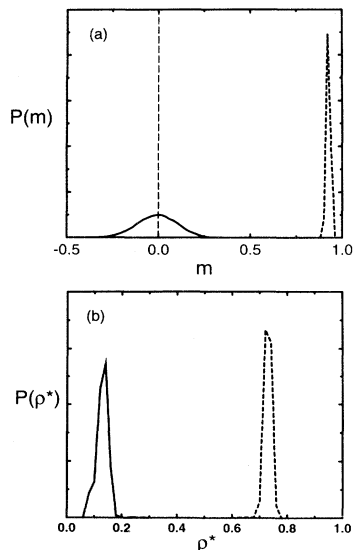


FIG. 3. Magnetization histogram (a) and density histogram (b) at the density of  $\bar{\rho}^* = 0.45$  and the temperature  $T^* = 0.35$ . The dashed line refers to box 1 and the solid line to box 2.

the low-density “shoulder” as well as to the high-density shoulder in the density histograms and taking the centers of the Gaussians as estimates for the coexistence densities. By evaluating the coexistence densities for several temperatures we finally obtain the GEMC coexistence densities in our system, see Fig. 4. The resulting GEMC phase diagram is represented in Fig. 4 by circles, together with the results of Ref. [11] obtained in the canonical ensemble. Using the standard technique [1] of locating the intersection point of the (i) “rectilinear diameter law” line, which yields an extrapolation of the line of equal density difference to the two phases as a function of temperature  $[(\rho_g + \rho_l)/2 = a + bT]$ , and of (ii) the extrapolation line for the order parameter as a function of temperature near the tricritical point ( $\rho_l - \rho_g = B(T_c - T)^{\beta_u}$  using a value of 1/4 for the “subsidiary” tricritical exponent [20]  $\beta_u$ ), we obtain the estimates  $T_c^* = 0.55 \pm 0.02$  for the tricritical temperature and  $\rho_c^* = 0.465 \pm 0.02$  for the tricritical density. As mentioned in [11] the mean field theory predicts too large a coexistence region which results in an overestimation of the liquid-gas tricritical temperature by 100%. The choice of the numerical value for  $\beta_u$  underlying the fitting procedure of the order parameter deserves some remarks. As noted by Mon and Binder [18], when the correlation length  $\xi$  exceeds the linear system size,  $\sqrt{V} \ll \xi$ , close to the (tri)critical point, one would expect the mean field exponent  $\beta_u^{MF}$  to be applicable, which in the case of a tricritical point in a two-dimensional system is  $\beta_u^{MF} = 1$  [21]. In the neighborhood of the tricritical point in a regime where  $\sqrt{V} \gg \xi$ , however, one should expect the true tricritical exponent for the infinite size system  $\beta_u$  to be valid. Besides conjectures [21] in favor of  $\beta_u = 1/4$ , MC renormalization group computations [22] yield an estimate for this value of  $\beta_u \approx 0.234$ . In the present study we chose the value  $\beta_u = 0.25$  for all temperatures. This procedure of using for all temperatures the same numerical value for the exponent was recently suggested [23] in the context of liquid-gas phase coexistence of a Lennard-Jones fluid, where a comparative study showed that with this procedure critical parameters can be obtained with an

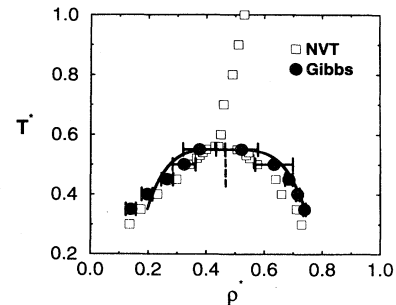


FIG. 4. Phase diagram for  $\omega_0/J = 4$ ,  $J = 1$ ,  $N = 200$ , and  $P/\beta J \approx 40$ . Circles represent results for the coexistence densities from this work, squares refer to the results of [11] (the squares for temperatures above the tricritical point mark the continuous ferroparamagnetic transition in the fluid phase). The line is a fit of the data to the scaling behavior  $[(\rho_l - \rho_g) = B(T_c - T)^{\beta_u}]$  using  $\beta_u = 1/4$  and the dashed line is the fit through the “rectilinear diameter data”  $[(\rho_g + \rho_l)/2 = a + bT]$ .

accuracy of 1% if data points in the immediate neighborhood of the critical point, where mean-field behavior occurs, are discarded. Deviations of the resulting fit curve for the order parameter from the data in Fig. 4 may be caused by this too small an exponent very close to the tricritical point. Finally we find only a weak ensemble dependency of the results within their statistical reliability: the GEMC values we obtained for  $T^*$  and  $\rho^*$  are in close agreement with the values of a previous canonical study [11] in conjunction with the block analysis of the order parameter. Thus using similar system sizes and computational resources, these two methodologies are competitive with respect to their capacity to efficiently obtain *rough* estimates for liquid-gas coexistence data and critical points in off-lattice systems.

In this paper we presented a combination of path-integral Monte Carlo and Gibbs-ensemble Monte Carlo simulation techniques for the investigation of phase transitions in mixed quantum-classical fluids. As a generic Hamiltonian, our model fluid had classical translational degrees of freedom in two spatial dimensions and internal quantum states. At low temperatures this system has a first-order phase transition with the coexistence of

a paramagnetic gas and a ferromagnetic liquid. Owing to the advantage of having immediate access to both coexisting phases without additional effort, one can easily evaluate thermal properties such as the internal and interaction energies or the magnetization without the disturbing interface present in canonical ensemble simulations. The coexistence densities at low temperatures and estimates for the tricritical point are obtained in good agreement with the results of a study using the canonical ensemble. We think that the combination of techniques presented here, PIMC and GEMC, may have a broad range of applications in future investigations of problems involving internal quantum states coupled with classical translations.

#### ACKNOWLEDGEMENTS

F.S. thanks the Deutsche Forschungsgemeinschaft (DFG) for support under Contract No. Ni-259/6-1. D.M. thanks the DFG for a Forschungsstipendium and IBM for financial support. P.N. thanks the DFG for support (Heisenberg foundation). The computations were carried out on the CRAY-YMP computer of the HLRZ at Jülich.

- [1] A.Z. Panagiotopoulos, *Mol. Phys.* **61**, 813 (1987).
- [2] B. Smit, Ph. De Smedt, and D. Frenkel, *Mol. Phys.* **68**, 931 (1989); B. Smit and D. Frenkel, *ibid.* **68**, 951 (1989).
- [3] A.Z. Panagiotopoulos, *Molec. Simul.* **9**, 1 (1992); B. Smit, in *Computer Simulation in Chemical Physics*, edited by M.P. Allen and D.J. Tildesley (Kluwer, Dordrecht, 1993), p. 173.
- [4] K. Binder, *Z. Phys. B* **43**, 119 (1981).
- [5] M. Rovere, D.W. Heermann, and K. Binder, *Europhys. Lett.* **6**, 585 (1988); *J. Phys. Condens. Matter* **2**, 7009 (1990); M. Rovere, P. Nielaba, and K. Binder, *Z. Phys. B* **90**, 215 (1993); H. Weber and D. Marx, *Europhys. Lett.* **27**, 593 (1994).
- [6] *Phase Transitions in Surface Films 2*, edited by H. Taub, G. Torzo, H.J. Lauter, and S.C. Fain, Jr. (Plenum, New York, 1991).
- [7] H. Wiechert and S.-A. Arlt, *Phys. Rev. Lett.* **71**, 2090 (1993).
- [8] O. Opitz, D. Marx, S. Sengupta, P. Nielaba, and K. Binder, *Surf. Sci. Lett.* **297**, L122 (1993); D. Marx, O. Opitz, P. Nielaba, and K. Binder, *Phys. Rev. Lett.* **70**, 2908 (1993); V. Pereyra, P. Nielaba, and K. Binder, *J. Phys. Condensed Matter* **5**, 6631 (1993); D. Marx, S. Sengupta, P. Nielaba, K. Binder, *Phys. Rev. Lett.* **72**, 262 (1994).
- [9] J.A. Barker, *J. Chem. Phys.* **70**, 2914 (1979); D. Chandler and P.G. Wolynes, *ibid.* **74**, 4078 (1981).
- [10] K.E. Schmidt and D.M. Ceperley, in *The Monte Carlo Method in Condensed Matter Physics*, edited by K. Binder, Springer Topics in Applied Physics Vol. 71 (Springer, Berlin, 1992).
- [11] D. Marx, P. Nielaba, and K. Binder, *Phys. Rev. Lett.* **67**, 3124 (1991); *Phys. Rev. B* **47**, 7788 (1993); S. Sengupta, D. Marx, and P. Nielaba, *Europhys. Lett.* **20**, 383 (1992); A.C. Mitus, D. Marx, S. Sengupta, P. Nielaba, A.Z. Patashinskii, and H. Hahn, *J. Phys. Condens. Matter* **5**, 8509 (1993).
- [12] D. Marx, *Surf. Sci.* **272**, 198 (1992); D. Marx, in *Computer Simulation Studies in Condensed-Matter Physics VI*, edited by D.P. Landau, K.K. Mon, and H.-B. Schüttler (Springer, Berlin, 1993).
- [13] R.M. Stratt, *J. Chem. Phys.* **80**, 5764 (1984); S.G. Desjardins and R.M. Stratt, *ibid.* **81**, 6232 (1984).
- [14] P. Ballone, P. de Smedt, J.L. Lebowitz, J. Talbot, and E. Waisman, *Phys. Rev. A* **35**, 942 (1987); P. de Smedt, P. Nielaba, J.L. Lebowitz, J. Talbot, L. Doooms, *ibid.* **38**, 1381 (1988).
- [15] F. Schneider (unpublished).
- [16] A typical run of  $10^6$  MC steps took about 14 CPU hours on a CRAY YMP; one MC step consisted of 200 attempted translational displacements, 20 particle exchange attempts, one volume change attempt and spin flip attempts of chain segments randomly varying in length from 1 to  $P$ .
- [17] J.I. Siepmann, I.R. McDonald, and D. Frenkel, *J. Phys. Condens. Matter* **4**, 679 (1992); J.R. Recht and A.Z. Panagiotopoulos, *Mol. Phys.* **80**, 843 (1993).
- [18] K.K. Mon and K. Binder, *J. Chem. Phys.* **96**, 6999 (1992); K.K. Mon, *Phys. Rev. B* **47**, 5497 (1993).
- [19] S. Sengupta, D. Marx, P. Nielaba, and K. Binder, *Phys. Rev. E* **49**, 1468 (1994).
- [20] R.B. Griffiths, *Phys. Rev. B* **7**, 545 (1973).
- [21] I.D. Lawrie and S. Sarbach, in *Phase Transitions and Critical Phenomena*, edited by C. Domb and J.L. Lebowitz (Academic, London, 1984), Vol. 9, see Sec. V.F and Table 5; note that  $\beta_2$  in this paper is identical to  $\beta_u$  of Ref. [20]
- [22] D.P. Landau and R.H. Swendsen, *Phys. Rev. Lett.* **46**, 1437 (1981); according to Ref. [20]  $\beta_u$  is related to the tricritical exponent  $\alpha_t = 0.89$  and the crossover exponent  $1/\phi_t = 1/0.47$  as  $\beta_u = (1 - \alpha_t)/\phi_t \approx 0.234$ , according to Ref. [21] is  $\beta_2 = \beta_u = (d - y_1^c)/y_2^c = [d - (1.8 \pm 0.02)]/(0.84 \pm 0.05) \approx 0.238$  in  $d = 2$  dimensions, the latter expression indicating a rather large error bar for  $\beta_u$ .
- [23] A.Z. Panagiotopoulos, *Int. J. Thermophys.* (to be published).